Spider Silk: Mother Nature's Bio-Superlens

James N Monks,[†] Bing Yan,[†] Nicholas Hawkins,[‡] Fritz Vollrath,[‡] and Zengbo Wang[*†].

[†]School of Electronic Engineering, Bangor University, LL57 1UT, Bangor, UK.

[‡]Department of Zoology, University of Oxford, OX1 3PS, Oxford, UK.

Supporting Information

ABSTRACT: It was recently discovered that transparent micro-spheres and cylinders can function as super-resolution lens (i.e superlens) to focus light beyond the diffraction limit. A number of high-resolution applications based on these lenses have been successfully demonstrated and span nanoscopy, imaging and spectroscopy. Fabrication of these superlenses, however, are often complex and require sophisticated engineering processes. Clearly an easier model candidate, such as a naturally occurring superlens, is highly desirable. Here, we report for the first time a biological superlens provided by Nature: the Minor Ampullate spider silk spun from the *Nephila* spider. This natural bio-superlens can distinctly resolve 100 nm features under a conventional white-light microscope with peak wavelength at 600 nm, attaining a resolution of λ/6 that is well beyond the classical limit. Thus our work opens a new door to develop biology-based optical systems that may provide a new solution to integrating optics in biological systems.

KEYWORDS: *Biological Superlens, Spider silk, Super-resolution, Nanoscopy, Photonic Nanojet*

In 1873, the German physicist Ernst Abbe established the resolution limit of optical microscopes: The minimum distance, *s*, between two structural elements to be imaged as two objects instead of one is given by $s = \lambda/(2NA)$, where λ is the wavelength of light and NA is the numerical aperture of the objective lens.[1] The physical origin for this limited resolution is related to optical diffraction and the loss of evanescent waves in the far field that carry high-spatial frequency subwavelength information of an object and decay exponentially with distance.

Since the late 1990s, research on super-resolution optical microscopy grew rapidly, owing to the emergence of meta-materials, nanophotonics, and plasmonics. Well-known examples include the Nobel Prize winning super-resolution fluorescence microscopy techniques,[2-4] the Pendry-Veselago superlens,[5, 6] and the Super-oscillatory lens[7]. These techniques are based on narrowband-lasers and will not operate under broadband white-light sources. Recently, it was discovered that small microspheres and cylinders can focus incident light beyond optical diffraction limit, a phenomenon known as 'photonic nanojet'.[8, 9] Based on this effect, we pioneered the microsphere nanoscopy technique which uses superlensing microspheres as imaging lens and a resolution of 50 nm was demonstrated for plasmonic samples under white light illumination.[10-12] For non-plasmonic samples, a typical resolution of 100 nm can be achieved.[12] This technique is label-free and has been verified and advanced since by a number of groups across the world, including for example the confocal microsphere nanoscopy,[12, 13] solid immersion microsphere nanoscopy,[14, 15] microfiber nanoscopy[16] and new designs of microsphere superlens.[17-19] For an overall view of latest development on the technique see a recent review [12].

Superlensing microsphere and microfibers can be manufactured via engineering processes including chemical synthesis and photolithography. These processes, however, are complex and inaccessible for non-professionals. Now bio-mining (searching Nature for suitable materials and models) led us to look for a naturally occurring superlens in spider silks, which are transparent in nature and have micron-scale cylinder structure. Our study demonstrates that Minor Ampullate spider silk spun by the *Nephila edulis* spider is an outstanding candidate. That silk can clearly resolve 100 nm features under a conventional white-light microscope, attaining a resolution of λ/6, which goes well beyond the diffraction limit **of** λ/2NA.

The concept of a natural bio-superlens is thus feasible and worthy further exploration. Here we provide our experimental setup followed by our imaging results and a discussion that is further supported by light scattering calculations.

Figure 1 shows the spider, its silk and the corresponding imaging experimental setup. The silk used in our experiments were Minor Ampullate glands filaments reeled directly from *Nephila edulis* spiders (Fig. 1a). Controlling spinning conditions allowed us to control the dimensions and mechanical properties of the threads.[20, 21] In this study, the spun silk filament had a diameter of 6.8 μm and refractive index of 1.55.[22] To facilitate manipulation and precision positioning of the silk at desired location, the silk

was top-encapsulated using a transparent cellulose-based tape and directly placed on top of the imaging sample surface. Isopropyl alcohol (IPA, refractive index 1.377) was then injected to fill the gap of silk and sample surface (Fig. 1b), as to improve the sample-silk contact and imaging constant. The sample systems were examined in reflection mode under a white light microscope equipped with a halogen lamp with peak wavelength at 600 nm (Olympus BX60). Two imaging samples were used: a semiconductor chip with features about 400-500 nm (above diffraction limit), and a commercial Blu-ray disk with 100/200nm features (below diffraction limit). The focusing property of spider silk was accurately simulated using CST Studio software, which is a full wave numerical solver of Maxwell equations based on Finite Integral Technique (FIT).[23]

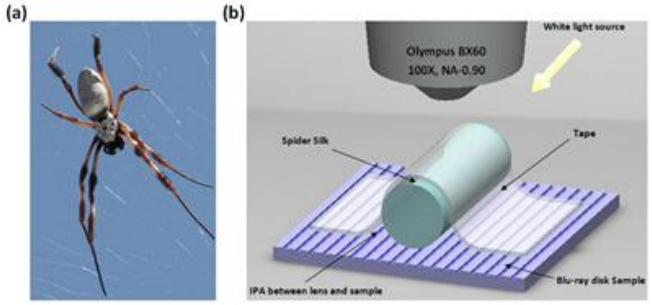

Figure 1. (a) *Nephila edulis* spider in its web. (b) schematic drawing of reflection mode silk bio-superlens imaging. The spider silk was placed directly on top of the sample surface by using a soft tape. The gaps between silk and sample was filled with IPA which improves imaging contrast. The silk lens collects the underlying near-field object information and projects a magnified virtual image into a conventional objective lens (100x, NA:0.9).

The silk lens is essentially a microfiber lens. As long as the lens is in close contact with imaging object, the near-field evanescent waves of objects can be picked up by the silk and transferred to the far-field objective lens. Such near-to-far field conversion leads to optical super-resolution and only occurs for small sized transparent spherical or cylindrical micro-lenses whose optical aberrations are small or negligible.[24] Typical diameter of these lenses are around 3 to 100 μm, with a best resolution of 50 nm demonstrated by us in 2011 for 5 – 10 μm microspheres.[10] Comparing to the spherical lens, which is an isotropic two-dimensional (2D) magnifying device, the cylindrical silk lens used in this study is expected to have different imaging characteristics - because a cylinder lens produces line-shaped focusing rather than the dot-spot focusing of a spherical case. Thus the cylindrical lens is essentially a 1D magnifying device that only magnifies objects along the direction perpendicular to the optical axis and hence provides an anisotropic magnifying device.

This 1D effect is demonstrated in Fig. 2(a-b), in which a semiconductor chip sample with line features 400-500 nm (Fig. 2a) was imaged with silk lens placed on top (Fig. 2b). Here, one can clearly see the silk generates a clear image of underlying line objects, but with a twisted angle. This twisted angle is the result of anisotropic magnification effect of cylindrical lens. Exact twist angle, as shown in the labels of Fig. 2(b) is slightly smaller than the twist angle of spider silk orientation with respect to the line objects, which is resulted by the angular incident beam used in the project. In fact, one may easily observe such angle-twisting effect at home, using a plastic bottle filled with water (as cylindrical lens) and any objects like drawing lines and shapes. The supplementary Material S1 provides further demonstration of the effect.

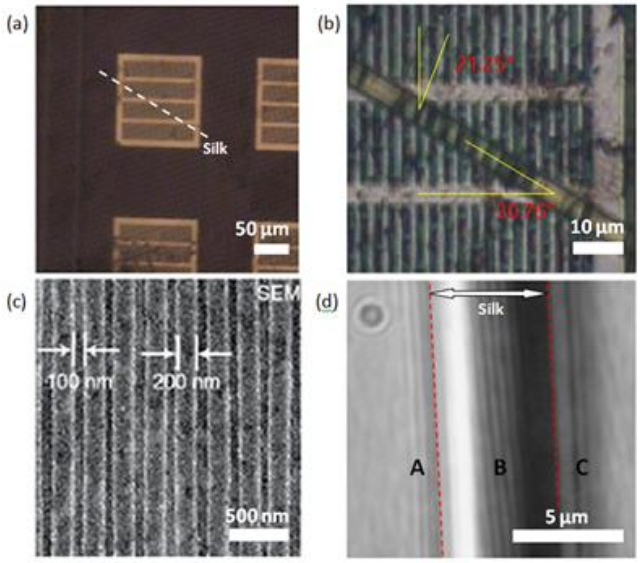

Figure 2. A typical imaging example of silk superlens nanoscope in reflection mode imaging a surface of an integrated circuit and commercial Blu-ray disk. The 100-μm thick transparent protection layer of the Blu-ray disk has been removed prior to using the minor ampullate spider silk (diameter of 6.8 μm). Micro dimensional integrated surface pattern (a; Optical imaging) is magnified by the spider silk (b; Optical Nanoscope image). The sub-diffraction 100 nm channels (c; SEM image) are resolved by the spider silk superlens (d; Optical Nanoscope image) and correspond to a magnification fact of 2.1X.

After measuring the basic imaging characteristics of microfiber lens, we proceeded to test the super-resolution imaging performance of the silk. A sub-diffraction Blu-ray disk (Fig. 2c) containing 200 nm and 100 nm features was used as the imaging objects. As expected, without silk, the microscope cannot resolve these features due to the optical diffraction limit (600/2NA= 333.3 nm, where NA=0.9). However, clearly magnified (M~2.1) super-resolution images could be obtained after carefully adjusting the illumination angle of the lighting; best images were obtained at roughly an angle of 20-40 degree measured from the vertical axis. This angular illumination effect can be observed in Fig. 2(d) image, on silk's left side a bright strip exists (Zone A) while on right side a dark strip appears (Zone C). Note that only images appearing inside the marked viewing windows (Zone B) are 'true' images of

underlying Blu-ray features, while the line images that appear in zone A and C are 'false' images. When a non-structured sample was used as the imaging specimen, the same phenomenon of 'false' images in Zone A and C was observed. This supports the hypothesis that 'false' images are not caused by the surface structures, but by the interferences between incident light, light scattered by the silk and reflection of the scattered light by substrates.[25, 26] Experimentally, the issue of 'true' or 'false' image can be verified by rotating the underlying sample, where the 'true' images will follow the rotation of sample while the 'false' images will not. Artificial images are an issue in microsphere/cylinder based super-resolution technology and one must pay attention to it in order to avoid wrong interpretation of experimental observations.

We further compared the super-resolution imaging of the silk superlens with a microsphere superlens as shown in Fig.3. Here, we used a Barium Titanate ($BaTiO_3$) microsphere, with a similar diameter to the spider silk and a refractive index of 1.9, which was placed next to the silk strand and then encased both spherical and cylindrical lenses with a Polydimethylsiloxane (PDMS). $BaTiO_3$ microspheres have the proven ability to resolve sub-diffraction patterns when immersed in liquid or PDMS,[12, 14, 15] as shown in Fig.3 where the 200 nm wide channels and the 100 nm separation lines are clearly distinguished. Because microsphere is an isotropic 2D magnifying lens, the image orientation in the central zone of the viewing window is perfectly aligned with the object orientations and there is no twisting angle effect.

Similar to Fig. 2d, the spider silk in figure 3 can also clearly resolve the 100/200nm patterns while under the reflection mode. But the spider silk projects the pattern at an angled image, i.e with the twisting effect as discussed above. The focal lens plane of the spider silk differs slightly from that of the microspheres, which explains why the microsphere images are slightly out of focus. One obvious advantage of spider silk is the fact that its viewing window is extended along the fiber. This can easily reach centimeters, which makes it potentially attractive for large-area super-resolution imaging. In principle, it is possible to rotate the encapsulated silk lens and capture super-resolution images at different angles (with respect to objects) from 0 to 180-deg; and then use a software system to process and analyze the images and thus construct a whole super-resolution image over squared centimeters scale. Technically, we may achieve this by attaching the silk superlens to a nano-resolution scanning head and integrate it with an optical microscope. Such image reconstruction will be the immediate focus of our next technical developments following on the present work. More complex nanostructures will be used in future studies.

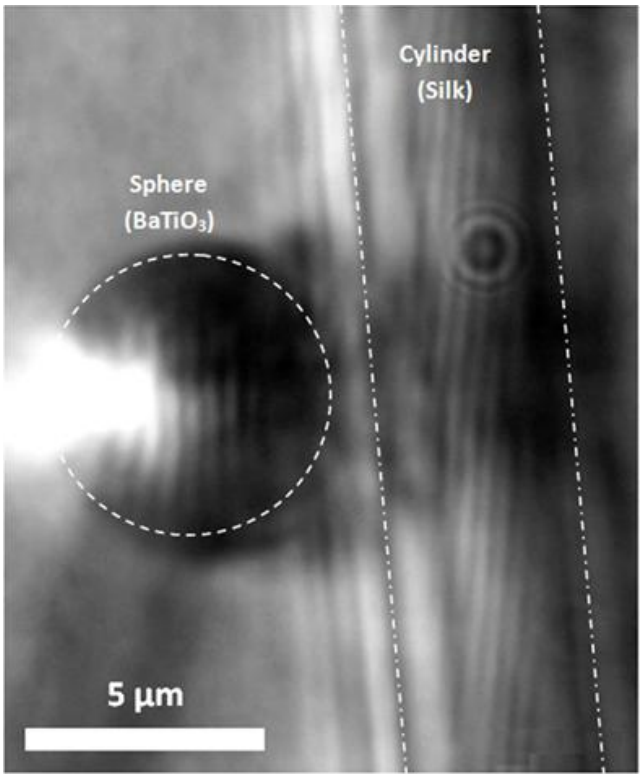

Figure 3. Microsphere positioned beside the minor ampullate spider silk in reflection mode, images a commercial Blu-ray disk. The image resolved within the spider silk is rotated by approximately four degrees compared to the real direct of the sub-diffraction 100 nm channels shown by the microsphere.

In our technique, super-resolution arises from the near-field interaction between the silk and underlying nano-objects, which leads to the conversion of surface-bounded high spatial frequency evanescent waves into propagating waves.[12, 27]. We note that such conversion process is extremely sensitive to the gap distance between silk and object. The technique requires gap distances below 100 nm with a zero distance gap being ideal.[12] In dry conditions, we failed to achieve super-resolution imaging with spider silk, most probably due to the poor contacting between silk and sample for an elongated object. Filling the gap zone with IPA helps eliminate the problem; a near-perfect contacting is formed due to capillary binding force occurring in the interfacial zone. Under an angular incident beam, the cylindrical spider silk lens produces an angled focus around 10 μm away from the lens (measured from lens centre), as shown in Fig.4. By varying the incident angle, the distance between object and lens (i.e, d and d' in Fig.4b) can be changed so that magnification factor M=f/(f-d) can be tuned. Generally, the magnification factor will increase with incident angle (see analysis in Fig. 4b) as d increases. However magnifications that are too large will cause the rapid decrease of imaging contrast, thus imposing a practical limit on the maximum

usable angle in experiments. Our tests show that 20-40 degree angles provide best results. A smaller sized spider silk may be used if a higher magnification of imaging is required.

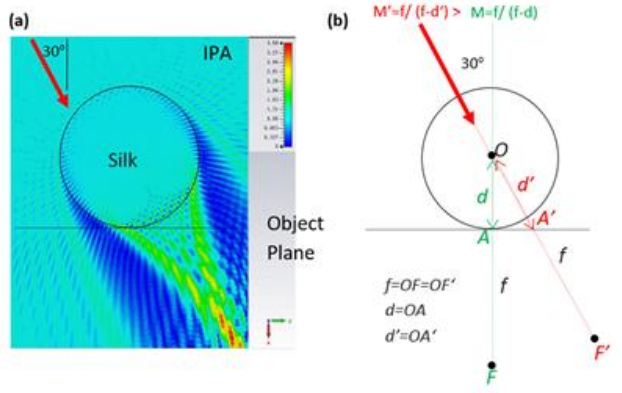

Figure 4. (a) Light focusing by the 6.8 μm-diameter minor ampullate spider silk immersed in IPA solution under a 600 nm wavelength illumination incident at 30 degree angle. (b) Schematics for magnification factor *M* calculation, the *M* generally increases with incident angle.

Theoretically the optical resonances in spherical cavity would cause variation of brightness and resolution in image versus wavelength and particle size. At some wavelengths or particle sizes such resonance could be quite sharp. However, these sharp resonances would be 'smeared' out by averaging effect when a broadband lighting source is used, such as the white lighting source used in our study. Such averaging effect was demonstrated previously when we tested wavelength effects using color filters, and confirmed the changes in brightness and resolution are not significant for red, green and blue lights [28]. In most cases such variations are almost negligible. It is the incident angle of light, which provided more significant conditions for determining the super-resolution image quality.

Our research reported here provides a solid foundation for the development of bio-superlens technology and it is the first expose of spider silk in this context. Now we expect further biological superlenses to be discovered. Indeed, interesting and important recent work by other researchers is heading in that direction. For example, Schuergers et al. reported that spherically-shaped cyanobacteria Synechocystis cells can focus light like a microlens, which contributes to the cell's ability to sense the direction of lighting source[29]. We suspect that these cells might work also as a superlens suitable for super-resolution imaging.

We conclude that the minor ampullate silk of the *Nephila edulis* spider, has the ability to perform as an optical superlens able to resolve subdiffraction 100-nm objects and patterns under a white light source illumination. This type of lens is the first biological superlens system that has successfully overcome the diffraction limit. The cylindrical silk lens has advantages in larger field-of-view when compared to microsphere superlens. Importantly for potential commercial applications, a spider silk nanoscope would be robust and economical, which in turn could provide excellent manufacturing platforms for a wide range of applications.

ASSOCIATED CONTENT

The supporting information is available free of charge on the ACS Publication website.
Demonstration of angle-twisting effect by cylindrical lens (Video S1) (AVI).

AUTHOR INFORMATION

Corresponding Author

* E-mail: z.wang@bangor.ac.uk

Notes
The authors declare no competing financial interest.

ACKNOWLEDGMENT

J.N.M, B.Y and Z.W acknowledge funding supports from Sêr Cymru National Research Networking Advanced Engineering and Materials, UK (NRN113) and Welsh Crucible Grant. F.V and N.H would thank funding support from US Air Force Office of Scientific Research AFOSR (FA9550-15-1-0264).

REFERENCES

(1) Abbe, E. *Archiv Microskop. Anat.* **1873,** 9, 413.
(2) Hell, S. W.; Wichmann, J. *Opt. Lett.* **1994,** 19, (11), 780-2.
(3) Betzig, E.; Patterson, G. H.; Sougrat, R.; Lindwasser, O. W.; Olenych, S.; Bonifacino, J. S.; Davidson, M. W.; Lippincott-Schwartz, J.; Hess, H. F. *Science* **2006,** 313, (5793), 1642-1645.
(4) Hess, S. T.; Girirajan, T. P. K.; Mason, M. D. *Biophys. J.* **2006,** 91, (11), 4258-4272.
(5) Pendry, J. B. *Phys. Rev. Lett.* **2000,** 85, 3966.
(6) Zhang, X.; Liu, Z. W. *Nat. Mater.* **2008,** 7, (6), 435-441.
(7) Rogers, E. T.; Lindberg, J.; Roy, T.; Savo, S.; Chad, J. E.; Dennis, M. R.; Zheludev, N. I. *Nat. Mater.* **2012,** 11, (5), 432-5.
(8) Chen, Z. G.; Taflove, A.; Backman, V. *Opt. Express* **2004,** 12, (7), 1214-1220.
(9) Lu, Y. F.; Zhang, L.; Song, W. D.; Zheng, Y. W.; Luk'yanchuk, B. S. *JETP Lett.* **2000,** 72, (9), 457-459.
(10) Wang, Z.; Guo, W.; Li, L.; Luk'yanchuk, B.; Khan, A.; Liu, Z.; Chen, Z.; Hong, M. *Nat. Commun.* **2011,** 2, 218.
(11) Wang, Z. B.; Li, L. *Laser Focus World* **2011,** 47, (7), 61-64.
(12) Wang, Z. B., Microsphere super-resolution imaging. In *Nanoscience*, Paual O Brien, J. T., Ed. Royal Society of Chemistry: 2016; Vol. 3, pp 193-210.

(13) Yan, Y.; Li, L.; Feng, C.; W.Guo; S.Lee; M.H.Hong. *Acs Nano* **2014,** 8, (2), 1809-1816.
(14) Darafsheh, A.; Walsh, G. F.; Dal Negro, L.; Astratov, V. N. *Appl. Phys. Lett.* **2012,** 101, (14), 141128
(15) Darafsheh, A.; Guardiola, C.; Palovcak, A.; Finlay, J. C.; Carabe, A. *Opt. Lett.* **2015,** 40, (1), 5-8.
(16) Darafsheh, A.; Wu, G.; Yang, S.; Finlay, J. C. In *Super-resolution optical microscopy by using dielectric microwires*, Three-Dimensional and Multidimensional Microscopy: Image Acquisition and Processing XXIII,, San Francisco, California, United States, 2016; Wilson, T. G. B. C. J. C. T., Ed. SPIE: San Francisco, California, United States, p 97130U
(17) Yan, B.; Yue, L. Y.; Wang, Z. B. *Opt. Commun.* **2016,** 370, 140-144.
(18) Yue, L. Y.; Yan, B.; Wang, Z. B. *Opt. Lett.* **2016,** 41, (7), 1336-1339.
(19) Fan, W.; Yan, B.; Wang, Z.; Wu, L. *Sci. Adv.* **2016,** 2, e1600901
(20) Vollrath, F.; Madsen, B.; Shao, Z. Z. *P Roy Soc B-Biol Sci* **2001,** 268, (1483), 2339-2346.
(21) Vollrath, F.; Knight, D. P. *Nature* **2001,** 410, (6828), 541-548.
(22) Little, D. J.; Kane, D. M. *Opt. Express* **2011,** 19, (20), 19182-19189.
(23) Weiland, T. *International Journal of Numerical Modelling* **1996,** 9, 295-319.
(24) Guo, H.; Han, Y.; Weng, X.; Zhao, Y.; Sui, G.; Wang, Y.; Zhuang, S. *Opt. Express* **2013,** 21, (2), 2434-43.
(25) Wang, Z. B.; Hong, M. H.; B.S.Luk'yanchuk; Y.Lin; Wang, Q. F.; Chong, T. C. *J. Appl. Phys.* **2004,** 96, 6845-6850.
(26) Wang, X. D.; Chen, B.; Wang, Z. S. *Opt. Laser. Eng.* **2012,** 50, (3), 349-353.
(27) Hao, X.; Kuang, C.; Gu, Z.; Wang, Y.; Li, S.; Ku, Y.; Li, Y.; Ge, J.; Liu, X. *Light: Science & Applications* **2013,** 2, (10), e108.
(28) Luk'yanchuk, B. S.; Arnold, N.; Huang, S. M.; Wang, Z. B.; Hong, M. H. *Appl. Phys. A* **2003,** 77, 209-215.
(29) Schuergers, N.; Lenn, T.; Kampmann, R.; Meissner, M. V.; Esteves, T.; Temerinac-Ott, M.; Korvink, J. G.; Lowe, A. R.; Mullineaux, C. W.; Wilde, A. *Elife* **2016,** 5.